Journal of ELECTRICAL ENGINEERING, VOL. 63, NO. 4, 2012, 213–223

STEADY–STATE ANALYSIS OF PARALLEL–OPERATED SELF–EXCITED INDUCTION GENERATORS SUPPLYING AN UNBALANCED LOAD

Jordan Radosavljević — Dardan Klimenta — Miroljub Jevtić *

This paper proposed a multi-objective genetic algorithm (MOGA) based approach for determining the steady-state performance characteristics of three-phase self-excited induction generators (SEIGs) operating in parallel and supplying an unbalanced load. The symmetrical component theory is used for the transformation of a complex three- phase generators-capacitances-load system to a simple equivalent circuit. The MOGA has been employed for the determination of unknown variables by minimizing the impedance module of the equivalent circuit. Using this approach, effects of various parameters on the terminal voltage control characteristics are examined for two parallel SEIGs with C2C connection under a single phase load.

K e y w o r d s: induction generator, self-excitation, parallel operation, voltage control, multi-objective genetic algorithm

List of symbols

R	resistance
X	reactance
F	frequency
v	rotor speed
$\mathcal{Z}$	impedance
$\mathcal{Y}$	admittance
C	capacitance
$\mathcal{U}$	complex voltage
$\mathcal{J}$	complex current
E_p	air-gap voltage
$\mathfrak{a}$	complex operator $e^{(j2\pi/3)}$

Subscripts

A, B, C	phases
WRM	wound rotor machine
SCM	squirrel cage machine
L	load
ℓ	line
s, r	stator and rotor
p, n	positive and negative sequence
m	magnetising
c	core loss
i	index

1 INTRODUCTION

The application of induction generators follows the development of distributed generation systems [1]. Advantages of induction generators in regard to widely applied synchronous generators are a lower unit cost, brush-less cage-rotor construction, absence of a separate dc source, good over-speed capability, better transient performances and inherent overload protection. The inability of a direct regulation of reactive power is a disadvantage of induction generators.

An induction generator can operate in parallel with the distribution network, when its rotor speed is greater than the synchronous speed of the air-gap revolving field. Better utilization of renewable energy may be achieved by developing small-scale autonomous power systems like wind and mini hydro power plants, which use the SEIGs [2]. Likewise, it is well known that if an appropriate capacitor bank is connected across an externally driven induction machine, an EMF is induced in the machine windings due to the excitation provided by the capacitor. The induced voltage and current would continue to rise, until the var supplied by the capacitor is balanced by the var demanded by the machine. This results in an equilibrium state being reached and the machine now operates as an SEIG at a voltage and frequency assigned by the value of the capacitance, speed of the prime mover, parameters of the machine and the load.

A huge number of journal publications has so far been dedicated to the steady-state analysis of an isolated three-phase SEIG with three-phase balanced load [3–14]. The performance of a SEIG is usually determined through its equivalent circuit. An overwhelming majority of the aforementioned researchers used either the loop impedance approach, or the nodal admittance approach in analyzing the circuit. Irrespective of the representation manner, the analysis of three-phase SEIG requires a computation of the generated frequency (F) and magnetizing reactance (X_m) for the given operating conditions. Knowing the values of X_m and F, the steady-state performance of the SEIG can easily be determined through their equivalent circuit in conjunction with appropriate magnetization characteristic.

Unbalanced operation of a three-phase SEIG may be caused by manufacturing tolerances of excitation capaci-

* Faculty of Technical Sciences, University of Priština in Kosovska Mitrovica, Kneza Miloša 7, 38220, Kosovska Mitrovica, Serbia, jordan.radosavljevic@gmail.com

DOI: 10.2478/v10187-012-0031-9, ISSN 1335-3632

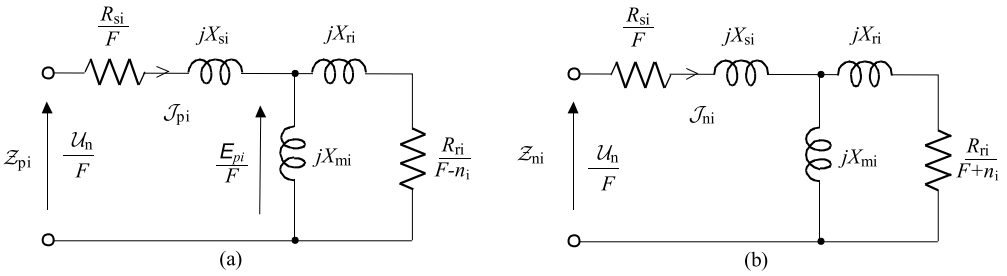

Fig. 1. Sequence equivalent circuits of the i^{th} induction machine: (a) positive sequence, (b) negative sequence

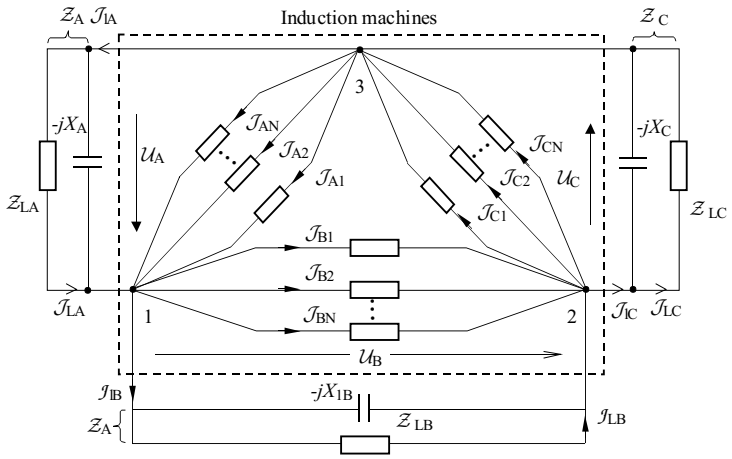

Fig. 2. N parallel SEIGs feeding a unbalanced load

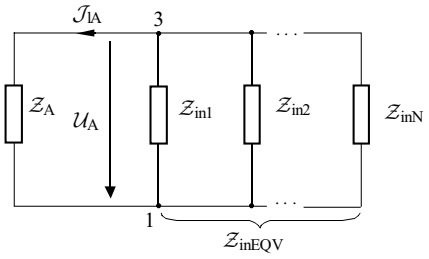

Fig. 3. A simplified circuit of N parallel SEIGs feeding a unbalanced load

tances, failure of some excitation capacitance modules or disconnection of loads by consumers [15]. The small-scale autonomous power system with a three-phase SEIG often supplies many single-phase loads, leading to a significant degree of load unbalance. In addition, such autonomous power systems usually employ single-phase distribution schemes due to a low cost, easy maintenance and simplicity in terms of protection. The steady-state analysis of three-phase SEIG with unbalanced loads and excitation capacitances is well documented [15–20].

In order to utilize the full potential of the hydro and wind energy source, a number of SEIGs are required to be operated in parallel. For parallel operation of SEIGs there was only a simplified model described in [21] and steady-state analysis in references [22–26]. These papers are focused on three-phase SEIGs with balanced excitation capacitances and loads. However, in practice, the conditions for symmetrical and balanced operation of three-phase SEIGs are often not achieved.

The steady-state analysis and performance characteristics of parallel operated three-phase SEIGs with unbalanced load conditions are not reported in literature. The aim of this paper is to contribute in this direction.

The key issue that needs to be solved at the parallel operated SEIGs is the voltage and frequency regulation. The voltage and frequency variables are nonlinearly dependent on the speeds, magnetizing reactances, excitation capacitances and loads. Any regulation strategy requires an efficient procedure for computing of the frequency and magnetizing reactances, that is, the steady-state condition of SEIGs.

In this paper, a MOGA-based optimization procedure is applied to the determination of the steady-state condition of any number parallel operated SEIGs feeding unbalanced load. The proposed approach enables practically all cases of unbalanced operation of the parallel SEIGs to be analyzed.

2 INDUCTION GENERATOR MODEL

If three-phase induction machines feed an unbalanced/asymmetrical external network, then a natural analysis mode is to resort the system to symmetrical components and rotating field concepts [2, 16]. Therefore, the induction generator is modeled with its positive and negative sequence circuits as it is shown in Fig. 1

In these circuits all parameters refer to the rated frequency, and it is assumed that all inductive reactances are proportional to the rated frequency; where F is the per-unit frequency — the ratio of the generated frequency to the rated frequency, and v_i is the ratio of the actual rotor speed to the synchronous speed corresponding to the rated frequency of the i^{th} machine. In these circuit models, it is also assumed that all parameters, except the magnetizing reactance X_{mi}, are constant and independent of the saturation. The value of X_{mi} depends

on the core flux which in turn depends on the ratio of the air-gap voltage to the frequency. The variation of the positive-sequence air-gap voltage with magnetizing reactance X_{mi} can be expressed by an appropriate equation based on the synchronous speed test data fitting.

According to Fig. 1, the positive-sequence and negative-sequence impedances of the i^{th} machine, that is, impedances $\mathcal{Z}_{pi}$ and $\mathcal{Z}_{ni}$, are as follows

$$\mathcal{Z}_{pi} = \frac{R_{si}}{F} + jX_{si} + \frac{jX_{mi}\left(\frac{R_{ri}}{F-v_i} + jX_{ri}\right)}{jX_{mi} + \left(\frac{R_{ri}}{F-v_i} + jX_{ri}\right)}, \quad (1)$$

$$\mathcal{Y}_{pi} = \mathcal{Z}_{pi}^{-1},$$

$$\mathcal{Z}_{ni} = \frac{R_{si}}{F} + jX_{si} + \frac{jX_{mi}\left(\frac{R_{ri}}{F+v_i} + jX_{ri}\right)}{jX_{mi} + \left(\frac{R_{ri}}{F+v_i} + jX_{ri}\right)}, \quad (2)$$

$$\mathcal{Y}_{ni} = \mathcal{Z}_{ni}^{-1},$$

where F is the per-unit frequency, v_i is the per-unit speed, R_{si} is the stator resistance per phase in pu, R_{ri} is the rotor resistance per phase referred to the stator in pu, X_{si} is the stator reactance per phase in pu, X_{ri} is the rotor reactance per phase referred to the stator in pu, and X_{mi} is the magnetizing reactance per phase at the rated frequency.

3 STEADY STATE ANALYSIS

The circuit connection of N three-phase delta connected SEIGs feeding a three-phase unbalanced load are shown in Fig. 2. Assigning appropriate values for the terminal impedances $\mathcal{Z}_A$, $\mathcal{Z}_B$ and $\mathcal{Z}_C$, a specific unbalanced operating condition can be simulated.

The delta connection is deliberately selected herein due to the fact that zero-sequence quantities do not exist. However, the presented concept can easily be extended to the star connection with the isolated neutral point applying the star-delta transformation.

The circuit shown in Fig. 2 has no active voltage sources. Accordingly, the SEIG may be regarded as a passive circuit when viewed across any two stator terminals [15]. For convenience, A–phase is chosen as the reference and the input impedance of the SEIGs across terminals 1 and 3 in Fig. 2 will be considered. In this manner, the equivalent scheme shown in Fig. 2 can be transformed into a simple circuit given in Fig. 3.

According to the marks given in Fig. 2, the current and voltage balance equations may be written as follows

$$\sum_{i=1}^{N} \mathcal{J}_{Ai} + \mathcal{J}_{\ell A} - \sum_{i=1}^{N} \mathcal{J}_{Bi} - \mathcal{J}_{\ell B} = 0\,, \quad (3)$$

$$\sum_{i=1}^{N} \mathcal{J}_{Ai} + \mathcal{J}_{\ell A} - \sum_{i=1}^{N} \mathcal{J}_{C} - \mathcal{J}_{\ell C} = 0\,, \quad (4)$$

$$\mathcal{J}_{\ell A} = \mathcal{Y}_A \mathcal{U}_A\,, \quad (5)$$

$$\mathcal{J}_{\ell B} = \mathcal{Y}_B \mathcal{U}_B\,, \quad (6)$$

$$\mathcal{J}_{\ell C} = \mathcal{Y}_C \mathcal{U}_C\,. \quad (7)$$

Based on the symmetrical component theory, the following equations are developed for the delta connected system

$$\mathcal{U}_A + \mathcal{U}_B + \mathcal{U}_C = 0, \quad (8)$$

$$\mathcal{U}_A = \mathcal{U}_p + \mathcal{U}_n\,, \quad (9)$$

$$\mathcal{U}_B = \mathfrak{a}^2 \mathcal{U}_p + \mathfrak{a}\mathcal{U}_n \quad (10)$$

$$\mathcal{U}_C = \mathfrak{a}\mathcal{U}_p + \mathfrak{a}^2 \mathcal{U}_n\,, \quad (11)$$

$$\sum_{i=1}^{N} \mathcal{J}_{Ai} = \mathcal{U}_p \sum_{i=1}^{N} \mathcal{Y}_{pi} + \mathcal{U}_n \sum_{i=1}^{N} \mathcal{Y}_{ni}\,, \quad (12)$$

$$\sum_{i=1}^{N} \mathcal{J}_{Bi} = \mathfrak{a}^2 \mathcal{U}_p \sum_{i=1}^{N} \mathcal{Y}_{pi} + \mathfrak{a}\mathcal{U}_n \sum_{i=1}^{N} \mathcal{Y}_{ni}\,, \quad (13)$$

$$\sum_{i=1}^{N} \mathcal{J}_{Ci} = \mathfrak{a}\mathcal{U}_p \sum_{i=1}^{N} \mathcal{Y}_{pi} + \mathfrak{a}^2 \mathcal{U}_n \sum_{i=1}^{N} \mathcal{Y}_{ni}\,. \quad (14)$$

This follows from equations (3) and (4)

$$\mathcal{J}_{\ell A} = -\sum_{i=1}^{N} \mathcal{J}_{Ai} + \sum_{i=1}^{N} \mathcal{J}_{Bi} + \mathcal{I}_{\ell B}\,, \quad (15)$$

$$\mathcal{J}_{\ell A} = -\sum_{i=1}^{N} \mathcal{J}_{Ai} + \sum_{i=1}^{N} \mathcal{J}_{Ci} + \mathcal{I}_{\ell C}\,. \quad (16)$$

Substituting equations (6, 7) and (12–14) into (15, 16), it is obtained that

$$\mathcal{J}_{\ell A} = \mathcal{A}\mathcal{U}_p + \mathcal{B}\mathcal{U}_n\,, \quad (17)$$

$$\mathcal{J}_{\ell A} = \mathcal{C}\,\mathcal{U}_p + \mathcal{D}\mathcal{U}_n \quad (18)$$

$$\mathcal{A} = (\mathfrak{a}^2 - 1)\sum_{i=1}^{N} \mathcal{Y}_{pi} + \mathfrak{a}^2 \mathcal{Y}_B\,, \quad \mathcal{B} = (\mathfrak{a} - 1)\sum_{i=1}^{N} \mathcal{Y}_{ni} + \mathfrak{a}\,\mathcal{Y}_B\,,$$

$$\mathcal{C} = (\mathfrak{a} - 1)\sum_{i=1}^{N} \mathcal{Y}_{pi} + \mathfrak{a}\mathcal{Y}_C\,, \quad \mathcal{D} = (\mathfrak{a}^2 - 1)\sum_{i=1}^{N} \mathcal{Y}_{ni} + \mathfrak{a}^2 \mathcal{Y}_C\,.$$

From equations (17) and (18), it is obtained that

$$\mathcal{U}_n = \frac{\mathcal{A} - \mathcal{C}}{\mathcal{D} - \mathcal{B}} \mathcal{U}_p\,. \quad (19)$$

According with Fig. 3, the phase voltage $\mathcal{U}_A$ is

$$\mathcal{U}_A = -\mathcal{Z}_{inEQV}\,\mathcal{J}_{\ell A}\,. \quad (20)$$

Finally, by substituting equations (9), (17) and (19) into equation (20), for the parallel SEIGs input impedance it is obtained that

$$\mathcal{Z}_{inEQV} = \frac{(\mathcal{A} + \mathcal{D}) - (\mathcal{B} + \mathcal{C})}{\mathcal{B}\mathcal{C} - \mathcal{A}\mathcal{D}}\,. \quad (21)$$

The positive-sequence and negative sequence admittances $\mathcal{Y}_{pi}$ and $\mathcal{Y}_{pi}$, that is the complex coefficients $\mathcal{A}$, $\mathcal{B}$, $\mathcal{C}$ and $\mathcal{D}$ are functions of F and X_{mi}. Therefore, the SEIGs input impedance may by expressed as

$$\mathcal{Z}_{inEQV} = R_{inEQV}\big(X_{m1}, X_{m2}, \ldots, X_{mN}, F\big) + jX_{inEQV}\big(X_{m1}, X_{m2}, \ldots, X_{mN}, F\big)\,. \quad (22)$$

In accordance with Fig. 3, the following voltage balance equation can be written

$$\big(\mathcal{Z}_A + \mathcal{Z}_{inEQV}\big)\mathcal{J}_{\ell A} = 0\,, \quad (23)$$

$$\mathcal{Z}_{loop}\mathcal{J}_{\ell A} = 0\,. \quad (24)$$

Where: $\mathcal{Z}_{loop} = \mathcal{Z}_A + \mathcal{Z}_{inEQV}$. For a successful self-excitation it is required that $\mathcal{J}_{\ell A} \neq 0$, hence,

$$\mathcal{Z}_{loop} = 0\,. \quad (25)$$

In order to ensure that all generators have the same terminal voltage (the common bus voltage), the following equations must be satisfied

$$|\mathcal{Z}_{p1}|\,|\mathcal{J}_{p1}| - |\mathcal{Z}_{pi}|\,|\mathcal{J}_{pi}| = 0 \quad (i = 2, \ldots, N)\,. \quad (26)$$

According to Fig. 1(a), the magnitude of the positive sequence stator current for machine i can be related to the machine magnetizing reactance X_{mi}, provided the relationship between the forward field air-gap voltage $\left|\frac{\mathcal{E}_{pi}}{F}\right|$ and magnetizing reactance X_{mi} is known. The magnetizing characteristic relating the $\left|\frac{\mathcal{E}_{pi}}{F}\right|$ with the X_{mi} can be obtained experimentally by a synchronous speed test. Generally, the variation of $\left|\frac{\mathcal{E}_{pi}}{F}\right|$ with X_{mi} over the practical region of operation can be approximated by linear segments with expressions of the type

$$\left|\frac{\mathcal{E}_{pi}}{F}\right| = a_i + b_i X_{mi} \quad (i = 1, \ldots, N)\,. \quad (27)$$

Therefore, equations (26) can be expressed as

$$\left|\frac{\mathcal{Z}_{p1}}{\mathcal{Z}_{pmr1}}\right|(a_1 + b_1 X_{m1})\left|\frac{\mathcal{Z}_{pi}}{\mathcal{Z}_{pmri}}\right|(a_i + b_i X_{mi}) = 0 \quad (i = 2, \ldots, N) \quad (28)$$

where $\mathcal{Z}_{pmri}$ is the total positive-sequence impedance of the magnetizing and rotor circuit of the i^{th} machine. In accordance with Fig. 1(a) it is

$$\mathcal{Z}_{pmri} = \frac{jX_{mi}\left(\frac{R_{ri}}{F - v_i} + jX_{ri}\right)}{jX_{mi} + \left(\frac{R_{ri}}{F - v_i} + jX_{ri}\right)}\,.$$

4 METHOD OF SOLUTION

If the self-excitation requirement (25) and voltage-balance equation (28) are treated as criterion functions and the frequency, magnetizing reactance, excitation capacitance and speed as control variables within the specified limits, then the multi-objective optimization procedure can be applied for the determination of the steady-state condition of three-phase SEIGs operating in parallel.

4.1 Objective functions

The equation (25) can be expressed as

$$f_1 = |\mathcal{Z}_{loop}| = 0\,. \quad (29)$$

The system of equations (28) is equivalent with following expression

$$f_2 = \sum_{i=2}^{N}\Big\{\Big|\frac{\mathcal{Z}_{p1}}{\mathcal{Z}_{pmr1}}\Big|(a_1 + b_1 X_{m1}) - \Big|\frac{\mathcal{Z}_{pi}}{\mathcal{Z}_{pmri}}\Big|(a_i + b_i X_{mi})\Big\} = 0\,. \quad (30)$$

The control of the common bus voltage can be achieved by changing in the excitation capacitances as well as changing rotor speeds of SEIGs. By controlling the voltage level one attain the voltage on the common bus of the SEIGs, that is, on the load which has the value equal to a previously specified one. This condition can be expressed with the objective function in the form

$$f_3 = \{|V_{spec} - V_t|\} = 0 \quad (31)$$

where: V_{spec} – specified voltage,
V_t – common bus voltage ($V_t = |\mathcal{U}_A|$).

Depending on the specific problem, a multi-objective function whose minimization leads to the determination of unknown variables at steady-state condition is created. The unknown variables, that is, optimization parameters can be magnetizing reactances (X_{mi}), frequency (F), excitation capacitance (C) and rotor speeds (v_i).

4.2 Multi-objective optimization

A general multi-objective optimization problem (MOP) can be defined as follows [27–30]

$$MinF(x) = [f_1(x), f_2(x), \ldots, f_k(x)]^{\top}$$
$$\text{s.t. } x \in S\,, \quad x = [x_1, x_2, \ldots, x_n]^{\top}$$

where $[f_1(x), f_2(x), \ldots, f_k(x)]$ are k objectives functions, $[x_1, x_2, \ldots, x_n]$ are the n optimization parameters, and $S \in R^n$ is the solution or parameter space.

For MOP, the optimal solution can be defined as the solution that is not dominated by any other solution in the search space. Such an optimal solution is called Pareto-optimal.

Pareto-optimal solution: x^* is said to be a Pareto-optimal solution of MOP if there exists no other feasible x (*ie* $x \in S$) such that, $f_j(x) \leq f_j(x^*)$ for all $j = 1, 2, \ldots, k$ and $f_j(x) < f_j(x^*)$ for at least one objective function f_j.

In solving an MOP, two conceptually distinct types of problem difficulty can be identified: search and decision-making. The first aspect refers to the optimization process in which the feasible set is sampled for Pareto-optimal solutions. The second aspect addresses the problem of selecting a suitable compromise solution from the Pareto-optimal set. A human decision maker is necessary to make the trade-offs between conflicting objectives. There are different ways to approach a MOP such as evolutionary algorithms. Evolutionary algorithms seem particularly suitable to solve MOP, because they deal simultaneously with a set of possible solutions (the so-called population). This allows finding several members of the Pareto- optimal set in a single run of the algorithm. The most local search method in MOP is GA. It has been proven that MOGA is intelligent optimization algorithm able to balance the trade-offs between conflicting objectives.

The classical optimisation methods start from a single possible initial solution and they reach the optimum by applying the heuristic rules iteratively. The MOGA starts from the population, which is a group of individuals. Each individual represents a potential solution of the optimization problem. The individuals are presented in the same way, usually through a column or a string of data. The quality of each solution or individual is determined based on the fitness function values. Through a series of MOGA operations a new population is obtained and its individuals are engendered by the individuals from the previous population according to the natural evolution principles: the choice of parents, crossover and mutation. Basic operations of the MOGA are:

1. Representation of individuals: All data (variables) that make an individual are written in a string. A string is composed of substrings. Each substring represents a binary encoded variable on which the process of optimisation is carried out. The number of substrings, therefore the size of a string, depends on the number of variables that are optimized.
2. Initialization: individuals with random strings are generated that set up the initial population.
3. Fitness function calculation: It is used to rate the quality of an individual and it represents an equivalent of the function that should be optimised, that is, objective function. The evaluation of the function is performed by the MATLAB program based on the mathematical model that is presented in sections 2 and 3.
4. Selection: During the selection process the individuals that will participate in the reproduction (parents) are selected. The point of the selection is to store and transfer good individuals to the next generation.
5. Crossover: Crossover is an exchange process of column parts between two individuals, that is, "parents". One or two new individuals engender by the crossover, that is, a "child". The possibility of inheriting the first parent's characteristics by a child is introduced during this process.
6. Mutation: Mutation is a way to give a new piece of information to an individual. Mutation represents an accidental bit variation of an individual, generally with a constant probability for each bit within a population. The mutation probability can further vary depending on the size of the population, application and preferences of the explorer. A fixed value which is often kept during the whole genetic algorithm is used for each generation.
7. Ending conditions: The process of finding the optimal solution is an iterative process which ends when a maximum number of generations is achieved or when another criterion is fulfilled, such as a minimum offset from the best fitness value and medium fitness value of all individuals in a current population. If end conditions are fulfilled, the best individual thus obtained is the semioptimal solution in question. Otherwise, return to 3.

In this paper, the MATLAB realization of the MOGA is applied. The MOGA parameters implemented in this paper are shown in Table 1.

Minimization of the above-formulated objective functions using the MOGA yield a set of Pareto-optimal solutions. For practical applications, it is need to select one solution. In this paper a simple principle is applied, that is, from the set of Pareto-optimal solutions should be choosing one that meets the following criteria

$$\min \sum_{i=1}^{k} f_i(x^*) \,. \tag{32}$$

4.3 Performance equations

The MOGA enables a simultaneous computation of the unknown values of X_{mi} and F. Having thus determined the X_{mi} and F, the next step is to determine the normalised air-gap voltage $\left|\frac{\mathcal{E}_{pi}}{F}\right|$ according to value of X_{mi} based on the relevant magnetizing characteristic for all induction machines. Because the phase angles of the normalised air-gap voltages are not known, it can be supposed that the angle of the SEIG with index 1 is equal to zero. Knowing the air-gap voltage $\mathcal{E}_{p1} = E_{p1}\angle 0°$, in accordance with Fig. 1(a), the positive-sequence current of the SEIG can be computed as

$$\mathcal{J}_{p1} = -\frac{\mathcal{E}_{p1}}{\mathcal{Z}_{pmr1}} \,. \tag{33}$$

Now, the positive-sequence voltage is

$$\mathcal{U}_p = \mathcal{E}_{p1} - (R_{s1} + jFX_{s1})\mathcal{J}_{p1} \,. \tag{34}$$

When $\mathcal{U}_p$ is calculated, the positive-sequence currents of the other SEIGs can be determined,

$$\mathcal{J}_{pi} = -\frac{\mathcal{U}_p}{F\mathcal{Z}_{pi}} \quad (i = 2, \ldots, N) \,. \tag{35}$$

Table 1. MOGA Parameters

Generation	200*(Number of variables)
Population	15*(Number of variables)
Initial population	Feasible population
Selection	Tournament, Tournament size: 2
Crossover	Heuristic, Ratio: 1.2
Mutation	Adaptive feasible
Ending conditions	Max generation: 200*(Number of variables) Termination tolerance on the function value: 10^{-4}

Table 2. Machines parameters

	R_s	R_r	X_s	X_r	$X_{\max}$
WRM	0.09175	0.06354	0.2112	0.2112	2.00
SCM	0.16543	0.09324	0.1060	0.1060	2.84

The phase angles of the normalised air-gap voltages of the other SEIGs:

$$\theta_i = \arctan \frac{\operatorname{Im}\left\{\frac{\mathcal{U}_p}{F} + \left(\frac{R_{si}}{F} + jX_{si}\right)\mathcal{J}_{pi}\right\}}{\operatorname{Re}\left\{\frac{\mathcal{U}_p}{F} + \left(\frac{R_{si}}{F} + jX_{si}\right)\mathcal{J}_{pi}\right\}} \ (i = 2, \ldots, N)\,. \tag{36}$$

The negative-sequence voltage $\mathcal{U}_n$ can be determined by Equation (19) and the negative-sequence currents in accordance with Fig. 1 (b) by equation

$$\mathcal{J}_{ni} = -\frac{\mathcal{U}_n}{F\mathcal{Z}_{ni}} \quad (i = 1, \ldots, N)\,. \tag{37}$$

Accordingly with Fig. 1(b)

$$\mathcal{E}_{ni} = \frac{jX_{mi}\left(\frac{R_{ri}}{F+v_i} + jX_{ri}\right)}{jX_{mi} + \left(\frac{R_{ri}}{F+v_i} + jX_{ri}\right)}\mathcal{I}_{ni} \ (i = 1, \ldots, N)\,. \tag{38}$$

Finally, the terminal voltages and stator currents of the SEIGs can be calculated by Eqs. (9–11) and (12–14), respectively; and the line currents by Eqs. (5–7)

The output power (P_{Geni}) and the input power (P_{Inpi}) of the i^{th} SEIG is

$$P_{Geni} = \operatorname{Re}\{\mathcal{U}_p\mathcal{J}_{pi}^* + \mathcal{U}_n\mathcal{J}_{ni}^*\} \quad (i = 1, \ldots, N)\,, \tag{39}$$

$$P_{Inpi} = \operatorname{Re}\left\{\frac{E_{pi}^2}{\frac{R_{ri}}{F-v_i} - jX_{ri}} + \frac{E_{ni}^2}{\frac{R_{ri}}{F+v_i} - jX_{ri}}\right\} \quad (i = 1, \ldots, N) \tag{40}$$

and reactive power requirement

$$Q_i = \operatorname{Im}\left\{\mathcal{U}_p\mathcal{J}_{pi}^* + \mathcal{U}_n\mathcal{J}_{ni}^*\right\} \quad (i = 1, \ldots, N)\,. \tag{41}$$

5 RESULTS AND DISCUSSIONS

The proposed procedure is tested on two three-phase, 380 V (line), four pole, delta connected, 1 kW induction machines. Namely, a wound rotor machine (WRM) and a squireel cage machine (SCM). The per-unit measured parameters of the two machines are given in the Table 2 [22].

The measured per-unit variations of the air-gap voltages $|E_p|/F$ based on a 220 V with X_m for the two machines approximated as follows over the practical range of interest.

For the WRM

$$\left|\frac{\mathcal{E}_p}{F}\right| = 1.0007 - 0.1741X_m \text{ for } X_m \le 1.3666\,,$$

$$\left|\frac{\mathcal{E}_p}{F}\right| = 1.4298 - 0.4881X_m \text{ for } 1.3666 < X_m \le 1.7707\,,$$

$$\left|\frac{\mathcal{E}_p}{F}\right| = 3.0192 - 1.3857X_m \text{ for } X_m > 1.7707\,.$$

For the SCM

$$\left|\frac{\mathcal{E}_p}{F}\right| = 2.4408 - 0.6080X_m \text{ for } X_m \le 2.3839\,,$$

$$\left|\frac{\mathcal{E}_p}{F}\right| = 3.4592 - 1.0352X_m \text{ for } 2.3839 < X_m \le 2.8116\,,$$

$$\left|\frac{\mathcal{E}_p}{F}\right| = 9.7841 - 3.2848X_m \text{ for } X_m > 2.8116\,.$$

5.1 Basic approach

For known values of the excitation capacitances (C_A, C_B, C_C), the load impedances $(\mathcal{Z}_{LA}, \mathcal{Z}_{LB}, \mathcal{Z}_{LC})$, the SEIGs speeds $(v_1, v_2, \ldots, v_N)$ and machines parameters, unknown values of the magnetizing reactance's $(X_{m1}, X_{m2}, \ldots, X_{mN})$ and frequency (F) can be determined by minimizing the following objective function

$$\min Fobj = \min\{f_1 + f_2\}$$

$$\text{subject to } \begin{cases} X_{mi}^{\min} \le X_{mi} \le X_{mi}^{\max}\,, & i = 1, \ldots, N\,, \\ F^{\min} \le F \le F^{\max}\,. \end{cases}$$

The steady-state analysis results of parallel operated SEIGs for the different connections of balanced/unbalanced resistive loads and excitation capacitances are presented in Tables 3–5. It is considered that the SEIGs have equal and constant speeds of 1.0 pu.

As shown in Table 5, WRM output power is less than the output of SCM. This is due to the rotor impedance ratio of the SEIGs. On the other hand, the reactive power of the WRM is significantly higher than the reactive power of the SCM due to smaller value of the magnetizing reactance. The result of it is that the phase current of the

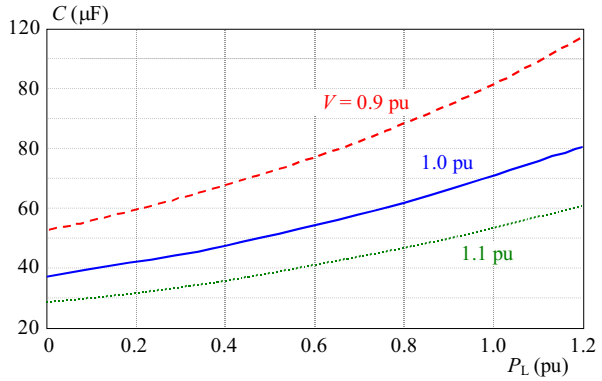

Fig. 4. Variation of C with P_L and v for a constant terminal voltage of $V_t = 1$ pu

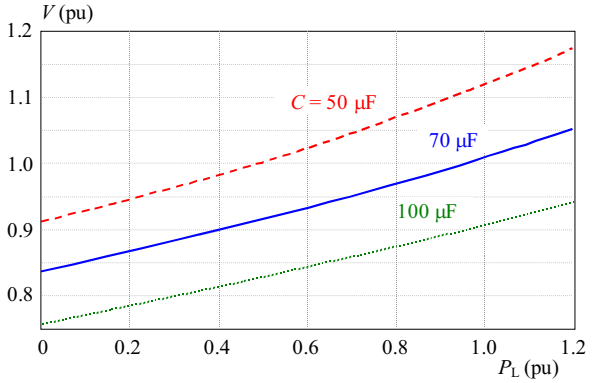

Fig. 7. Variation of v with with P_L and C for a constant terminal voltage of $V_t = 1$ pu

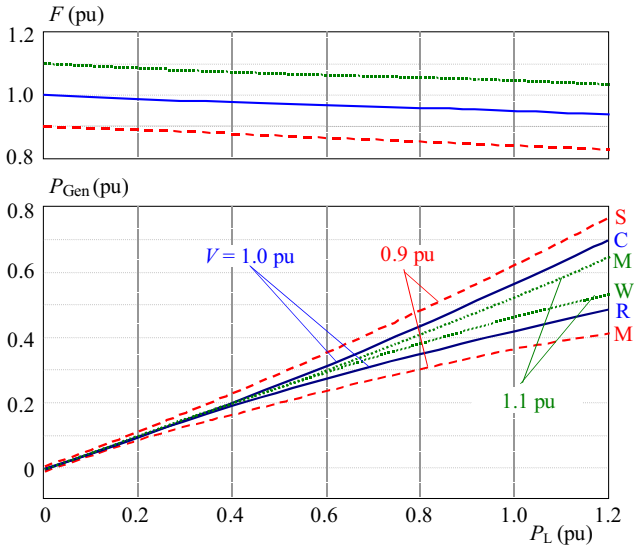

Fig. 5. Variation of F and P_{Gen} with P_L and v for a constant terminal voltage of $V_t = 1$ pu

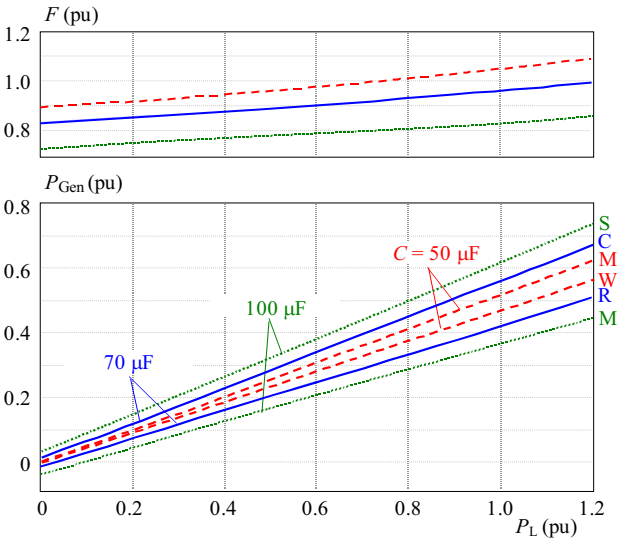

Fig. 8. Variation of F and Pgen with PL and C for a constant terminal voltage of Vt=1 pu

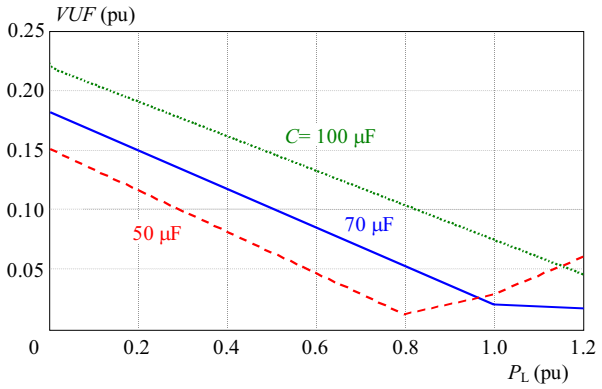

Fig. 6. Variation of VUF with P_L and v for a constant terminal voltage of $V_t = 1$ pu

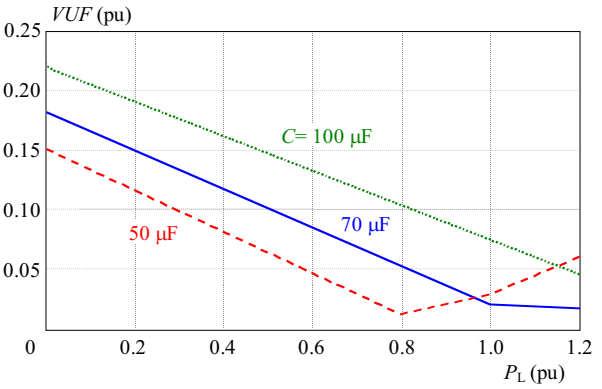

Fig. 9. Variation of VUF with PL and C for a constant terminal voltage of Vt=1 pu

WRM is significantly higher than the phase current of the SCM, as can be seen in Table 4. This clearly shows the importance of the parameters of the individual SEIGs in parallel operation.

The poor generator performance, such as phase imbalance and poor efficiency, will result when single-phase loads are supplied by three-phase SEIGs (cases 6 and 7). This disadvantage are overcome to a large extent by the use of the C2C connection (case 8).

This approach has been applied for C2C connection. Fig. 4 shows the variation of excitation capacitance C required to maintain the constant terminal voltage of $V_t = 1$ pu with the change in the resistive load P_L at the constant generators speeds v for the C2C connection. The excitation capacitance has to vary continuously in order to keep the terminal voltage at a constant value. From this figure, it is clear that C increases with P_L. For fixed values of V_t and P_L, C increases as v is decreased.

Table 3. Case studies for the different circuit configurations

Case	Note	$\mathcal{Z}_A \leftarrow R_{LA}\|\|C_A$		$\mathcal{Z}_B \leftarrow R_{LB}\|\|C_B$		$\mathcal{Z}_C \leftarrow R_{LC}\|\|C_C$		Results			
		R_{LA} (Ω)	C_A μF	R_{LB} (Ω)	C_B μF	R_{LC} (Ω)	C_C μF	F (pu)	X_m (pu) WRM	X_m (pu) SCM	$\min \sum_{i=1}^{k} f_i(x^*)$
1	Bal. Load; Bal. Cap.	100	60	100	60	100	60	0.9578	0.9314	2.3093	1.3234e-007
2	No Load; Bal. Cap.	–	40	–	40	–	40	0.9964	1.1409	2.4590	3.8158e-008
3	Bal. Load; Unbal. Cap.	100	50	100	60	100	70	0.9576	0.9313	2.3087	3.4803e-007
4	Unbal. Load; Bal. Cap.	50	60	100	60	150	60	0.9522	1.0554	2.3729	4.4291e-007
5	Unbal. Load; Unbal. Cap.	50	50	100	60	150	70	0.9522	1.0334	2.3593	7.4905e-007
6	Single-ph. Load; Bal. Cap.	33	60	–	60	–	60	0.9620	0.9417	2.3283	2.9628e-007
7	Plain single-ph. connection	33	180	–	–	–	–	0.9386	1.8268	2.7899	7.0679e-008
8	C-2C connection	33	60	–	120	–	–	0.9551	0.9356	2.3043	8.9868e-007

Table 4. Phase voltage, voltage unbalance factor and currents for the circuit configurations listed in Table 3

Case	V_A (pu)	V_B (pu)	V_C (pu)	VUF (V_n/V_p)	I_A (pu WRM	I_A (pu SCM	I_B (pu WRM	I_B (pu SCM	I_C (pu WRM	I_C (pu SCM	$I_{\ell A}$ (pu)	$I_{\ell B}$ (pu)	$I_{\ell C}$ (pu)
1	0.9715	0.9715	0.9715	0	1.1194	0.6645	1.1194	0.6645	1.1194	0.6645	1.7584	1.7584	1.7584
2	0.9460	0.9460	0.9460	0	0.7050	0.3734	0.7050	0.3734	0.7050	0.3734	1.0782	1.0782	1.0782
3	0.9437	0.9946	0.9764	0.0305	1.0464	0.6257	1.1458	0.6172	1.1756	0.7696	1.4773	1.8000	2.0130
4	0.8881	0.9017	0.9718	0.0572	1.0665	0.8260	0.9398	0.5091	1.1753	0.7375	1.9802	1.6244	1.6622
5	0.8700	0.9321	0.9844	0.0712	1.0193	0.8116	0.9822	0.4576	1.2452	0.8401	1.7735	1.6791	1.9414
6	0.8636	0.9596	1.1070	0.1486	1.0198	0.9729	0.8662	0.1190	1.4382	0.9714	2.4440	1.5840	1.8274
7	0.5672	0.3412	0.6403	0.3439	0.9977	1.0313	0.3530	0.6793	0.6779	0.3959	3.0350	0	0
8	0.9939	0.9733	0.9364	0.0346	1.1665	0.6327	1.2020	0.8065	1.0551	0.6468	2.8059	3.1905	0

Table 5. Output powers and efficiency for the circuit configurations listed in Table 3

Case	Power load P_L (pu)	P_{Gen} (pu) WRM	P_{Gen} (pu) SCM	Efficiency WRM	Efficiency SCM	Q_i (pu) WRM	Q_i (pu) SCM
1	0.7159	0.3239	0.3920	70.6876	80.7330	−1.0381	−0.5129
2	0	−0.0092	0.0092	25.0589	28.3383	−0.6669	−0.3531
3	0.7164	0.3247	0.3917	70.5678	80.3282	−1.0416	−0.5159
4	0.7637	0.3620	0.4017	73.9621	79.0921	−0.9075	−0.4793
5	0.7659	0.3617	0.4042	73.2110	78.3864	−0.9388	−0.4937
6	0.5715	0.2756	0.2958	67.3593	70.9987	−1.0499	−0.5414
7	0.2465	0.1541	0.0924	71.4587	46.8577	−0.3032	−0.2150
8	0.7569	0.3430	0.4139	70.7812	79.8785	−1.0504	−0.5243

The variations of frequency F and output powers of generators P_{Gen}, with load P_L at the corresponding values of the excitation capacitance are shown in Fig. 5. With an increase in load, the frequency is decreases. The range of change in frequency is approximately the same for all three speeds. The power load must be equal to the sum of output powers of parallel operated SEIGs. Figure 5 clearly shows that the power output of SCM generator is greater than the output power of WRM generator, although they have the same rated power. For fixed values of Vt and PL, the ratio of the output powers is increases as v is decreased.

Figure 6 shows the variation of the voltage unbalanced factor VUF with load P_L . For fixed values of $v = 0.9$ pu and $v = 1.0$ pu, VUF decreases as P_L increases. For generators speed of $v = 1.1$ pu, VUF decreases as P_L increases from 0 to 0.8 pu, and VUF increases as P_L increases from 0.8 to 1.2 pu Generaly, for fixed values of V_t and P_L, VUF decreases as v is increased. The minimum values of VUF depends on the speed. With increasing speed, the minimum of VUF moves to the left (toward smaller P_L).

5.2 Controlling terminal voltage by excitation capacitance

It is well known that the voltage control of the SEIG can be achieved by a change in the excitation capacitance for constant values of the speeds and load impedances. In

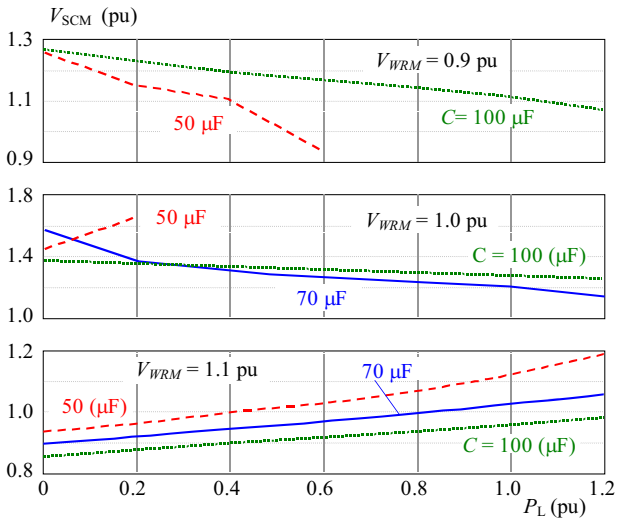

Fig. 10. ariation of v_{SCM} with P_P, C and v_{WRM} for a constant terminal voltage of $V_t = 1$ pu

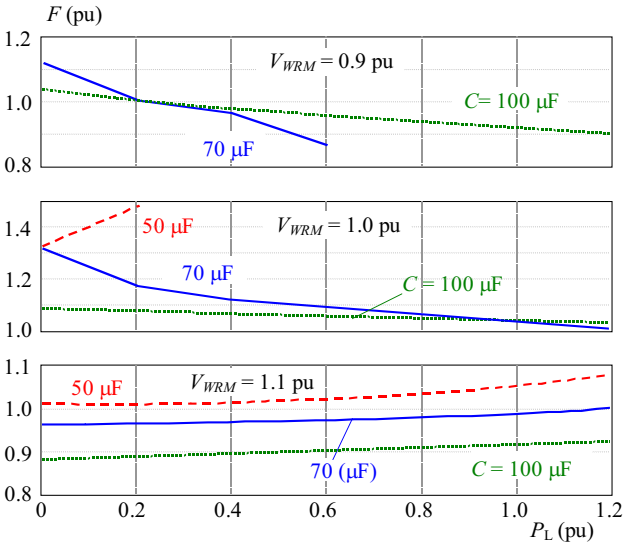

Fig. 11. Variation of F with P_P, C and v_{WRM} for a constant terminal voltage of $V_t = 1$ pu

this case the multi-objective function can be expressed as

$$\min Fobj = \min\{f_1 + f_2 + f_3\}$$

$$\text{subject to} \begin{cases} X_{mi}^{\min} \le X_{mi} \le X_{mi}^{\max}, & i = 1, \ldots, N, \\ F^{\min} \le F \le F^{\max}, \\ C^{\min} \le C \le C^{\max}. \end{cases}$$

5.3 Controlling terminal voltage by SEIGs speeds

For a fixed value of C, it may be possible to achieve a certain degree of voltage regulation by varying the speed of one or more machines [21]. In this situation, two cases can be analyzed: i) all SEIGs have common but variable speeds, and ii) the speed of only one SEIG is varied while keeping the speeds of the remaining $(N-1)$ SEIGs fixed. There can also be used multi-objective function

$$\min Fobj = \min\{f_1 + f_2 + f_3\}$$

$$\text{subject to} \begin{cases} X_{mi}^{\min} \le X_{mi} \le X_{mi}^{\max}, & i = 1, \ldots, N, \\ F^{\min} \le F \le F^{\max}, \\ v_i^{\min} \le v_i \le v_i^{\max}, & i = 1, \ldots, N. \end{cases}$$

(i) C2C connection, both SEIGs have common but variable speeds

Figure 7 shows the variation of SEIGs speeds v required to maintain the constant terminal voltage of $V_t = 1$ pu with the change in the resistive load P_L at the constant excitation capacitance C. The SEIGs speeds has to vary continuously in order to keep the terminal voltage at a constant value. From this figure, it is clear that v increases as P_L increases. For fixed values of V_t and P_L, v decreases as C is increased.

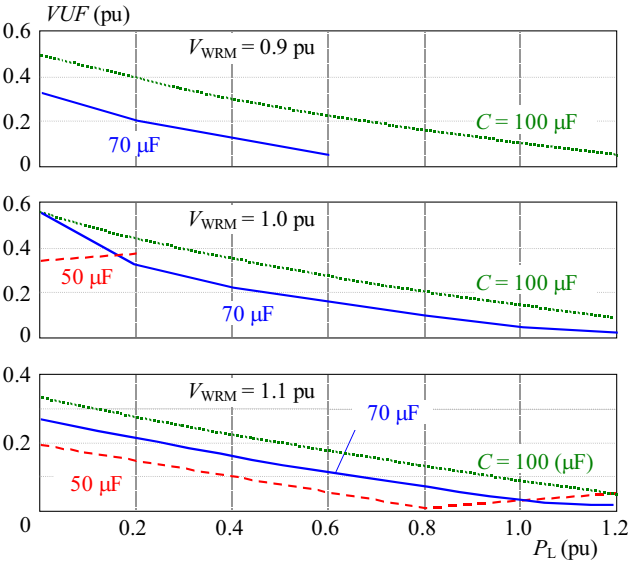

Fig. 12. Variation of VUF with P_L ,C and v_{WRM} for a constant terminal voltage of $V_t = 1$ pu

The variations of frequency F and output powers of generators P_{Gen}, with load P_L at the corresponding values of the generators speeds v are shown in Fig. 8.

With an increase in load, the frequency is increases. The range of change in frequency is approximately the same for all three excitation capacitances. As shown in Fig. 8 the power output of SCM generator is higher than the output power of WRM generator. The ratio of output powers SCM/WRM decreases as P_L increases. For fixed values of V_t and P_L, the ratio of the output powers increases as C is increased.

The effect of C on the VUF under voltage control by v is shown in Fig. 9. For fixed values of $C = 50\,\mu$F and $C = 70\,\mu$F, VUF is decreases as P_L increases. For $C = 100\,\mu$F, VUF decreases as P_L increases from 0 to 0.8 pu, and VUF increases as P_L increases from 0.8 to 1.2 pu Generally, for fixed values of V_t and P_L, VUF

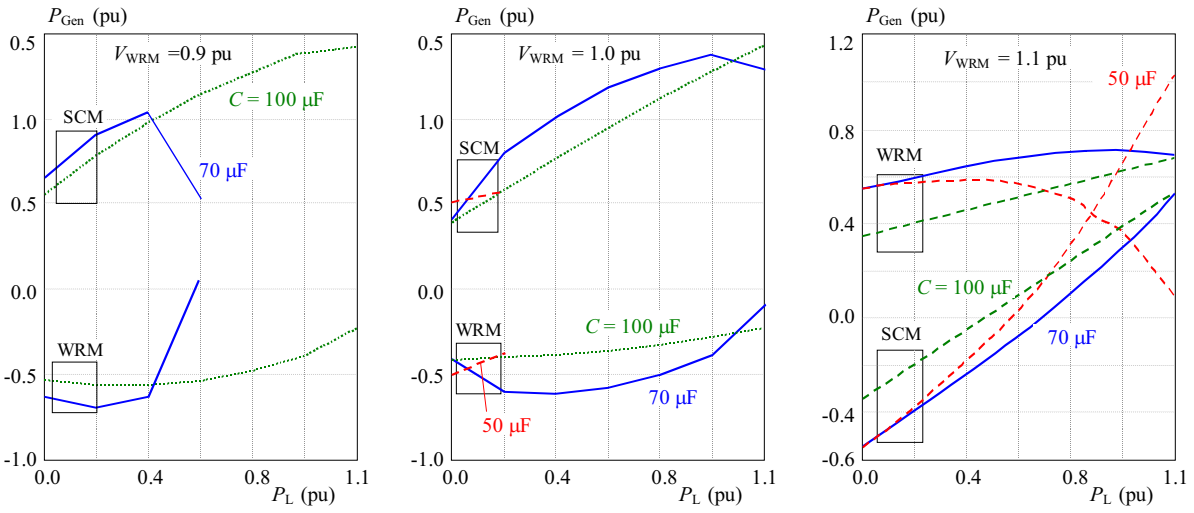

Fig. 13. Power outputs of SEIGs with P_L, C and v_{WRM} for a constant terminal voltage of $V_t = 1$ pu

decreases as C is decreased. With decreasing C, the minimum of VUF moves to the left (toward smaller P_L).

(ii) C2C connection, v_{SCM} is variable and v_{WRM} is kept constant

For the C2C connection SEIGs parallel system of an SCM and a WRM, voltage control by the speed of SCM is illustrated in Figs. 10–13. Based on these results it is clear that voltage control by the speed of only one machine is generally possible, but very limited.

Figure 10 shows the variation of the speed of the SCM (v_{SCM}) required to maintain the constant terminal voltage of $V_t = 1$ pu with the change in the resistive load P_L at the constant excitation capacitance C and the constant speed of the WRM (v_{WRM}). The v_{SCM} has to vary continuously in order to keep the V_t at a constant value. From this figure, it is clear that the v_{SCM} control characteristics largely depends on values of P_L, C and v_{WRM} . Generally, the control characteristics improves as v_{WRM} and C is increased. However, as can be seen from Figs. 13(a,b), the WRM output power is negative in over range of P_L, which means that the WRM operate as motor. For $v_{WRM} = 1.1$ pu, as shown in Fig. 13(c), the SCM operate as motor or generator depending on P_L and C. For fixed value of P_L the operating mode of SCM greatly depends upon the C. In addition to the value of P_L, C and v_{WRM}, the control caracteristics is highly dependent on the SEIGs parameters.

6 CONCLUSIONS

A multi objective genetic algorithm-based approach to evaluation the steady-state performance of three-phase SEIGs operated in parallel under unbalanced and single-phase load conditions is presented. The complex three-phase induction generators-excitation capacitance-load system is transformed to a simple equivalent circuit by using the symmetrical component theory. The MOGA has been applied to the computation of the unknowns by minimizing the multi-objective function which includes the self-excitation requirement, voltage balance for parallel operation and common bus voltage control criterion. Application of the MOGA gives great freedom in the choice of objective function and control variables in the analysis of the parallel operated SEIGs.

The voltage control of the parallel operated SEIG feeding an unbalanced load has been investigated as well. The methodology for voltage control has been implemented for C2C connection under single-phase load. From this results it is clear that the voltage control can be achieve by varying the excitation capacitance or by varying the common speeds of the SEIGs. The voltage control by varying the speed of only one SEIG is generally possible, but very limited. In addition to the excitation capacitance and speeds of the SEIGs, the voltage control characteristics is highly dependent on the induction machine parameters.

The proposed approach enables practically all cases of unbalanced operation of the parallel SEIGs to be analyzed. The methodology proposed in this paper can be exploited in planning and development of power generation in autonomous small-scale power plant with the SEIGs.

Acknowledgement

This paper presents the part of results of the Project TR 33046 funded by the Ministry of Science and Technological Development of the Republic of Serbia.

References

[1] RADOSAVLJEVIĆ, J.—JEVTIĆ, M. Klimenta,D.—: Optimal Seasonal Voltage Control in Rural Distribution Networks with Distributed Generators, J. Electrical Engineering **61** No. 6 (2010), 321–331.

[2] SIMOES, M. G.—FARRET, F. A.: Renewable Energy Systems – Design and Analysis with Induction Generators, CRC Press, Raton, FL, 2004.

[3] SHRIDHAR, L.—SINGH, B.—JHA, C. S.—SINGH, B. P.: Analysis of Self Excited Induction Generator Feeding Induction Motor, IEEE Transactions on Energy Conversion, **9** No. 2, (1994), 390–396.

[4] CHAN, T. F.: Steady-State Analysis of Self-Excited Induction Generators, IEEE Transactions on Energy Conversion **9** No. 2 (1994), 288–296.

[5] CHAN, T. F.: Self-Excited Induction Generators Driven by Regulated and Unregulated Turbines, IEEE Transactions on Energy Conversion **11** No. 2 (1996), 338–343.

[6] CHAKRABORTY, C.—BHADRA, S. N.—CHA-TTOPADHYAY, A. K.: Excitation Requirements for Stand Alone Three-Phase Induction Generator, IEEE Trans. on Energy Conversion **13** No. 4 (1998), 358–365.

[7] ALGHUWAINEM, S. M.: Steady-State Analysis of a Self-Excited Induction Generator Including Transformer Saturation, IEEE Transactions on Energy Conversion **14** No. 3 (1999), 667–672.

[8] ALOLAH, A. L.—ALKANHAL, M. A.: Optimization-Based Steady State Analysis of Three Phase Self-Excited Induction Generator, IEEE Trans. On Energy Conversion, **15** No. 1 (2000), 61–65.

[9] NIGIM, K. A.—SALAMA, M. M. A.—KAZERANI, K.: Identifying Machine Parameters Influencing the Operation of the Self-Excited Induction Generator, Electric Power Systems Research **69** (2004), 123–128.

[10] JOSHI, D.—SANDHU, K. S.: Performance Analysis of Three-Phase Self-Excited Induction Generator using Genetic Algorithm, Electric Power Components and Systems **34** (2006), 461–470.

[11] HAQUE, M. H.: Comparison of Steady State Characteristic of Shunt, Short-Shunt and Long-Shunt Induction Generators, Electric Power System Research **79** (2009), 1446–1453.

[12] HAQUE, M. H.: A Novel Method of Evaluating Performance Characteristics of a Self-Excited Induction Generator, IEEE Transactions on Energy Conversion **24** No. 2 (2009 pp 358–365).

[13] KUO, S. C.—WANG, L.: Steady-State Performance of a Self-Excited Induction Generator Feeding an Induction Motor, Electric Power Components and Systems **30** (2002), 581–593.

[14] ALOLAH, A. I.—ALKANHAL, M. A.: Analysis of Three Phase Self-Excited Induction Generator under Static and Dynamic Loads, Electric Machines & Drives Conference IEMDC '07, vol. 2, IEEE International Publication 2007, pp. 1783–1786.

[15] CHAN, T. F.—LAI, L. L.: Steady-State Analysis and Performance of a Stand-Alone Three Phase Induction Generator with Asymmetrically Connected Load Impedances and Excitation Capacitances, IEEE Transaction on Energy Conversion **16** No. 4 (2001), 327–333.

[16] MURTHY, S. S.—SINGH, B.—GUPTA, S.—GULATI, B. M.: General Steady-State Analysis of Three-Phase Self-Excited Induction Generator Feeding Three-Phase Unbalanced Load/Single-Phase Load for Stand-Alone Applications, IEE Proc. – Gener. Transm. Distrib. **150** No. 1 (2003), 49–55.

[17] ALOLAH, A. I.—ALKANHAL, M. A.: Excitation Requirements of Three Phase Self-Excited Induction Generator under Single Phase Loading with Minimum Unbalance, Power Engineering Society Winter Meeting, vol. 1, IEEE, 2000, pp. 257-259.

[18] KUMARESAN, N.: Analysis and Control of Three-Phase Self-Excited Induction Generators Supplying Single-Phase AC and DC Loads, IEE Proc. Electric Power Applications **152** No. 3 (2005), 739–747.

[19] WANG, Y. J.: Analysis of a Self-Excited Induction Generator Supplying Unbalanced Loads, International Conference on Power System Technology - POWERCON 2004, Singapore, 21-24 Nov 2004, pp. 1457–1462.

[20] IDJDARENE, K.—REKIOUA, D.—REKIOUA, T.—TOUNZI, A.: Performance of an Isolated Induction Generator under Unbalanced Loads, IEEE Transactions on Energy Conversion **25** No. 2 (2010), 303–311.

[21] WATSON, D. B.—MILNER, I. P.: Autonomous and Parallel Operation of Self-Excited Induction Generators, Int.J. Elect. Eng. Education **22** (1985), 365–374.

[22] Al-BAHRANI, A. H.—MALIK, N. H.: Voltage Control of Parallel Operated Self-Excited Induction Generators, IEEE Trans. Energy Conversion **8** (1993), 236-242.

[23] ALBAHRANI, A. H.—MALIK, N. H.: Steady State Analysis of Parallel Operated Self-Excited Induction Generators, Proc. Inst. Elect. Eng. C, **140,** No. 1, (1993), 49–55.

[24] LEE, C.-H.—WANG, L.: A Novel Analysis of Parallel Operated Self-Excited Induction Generators, IEEE Trans. Energy Conversion **13** No. 2 (1998), 117–123.

[25] CHAKRABORTY, C.—BHADRA, S. N.—CHATTOPADHYAY, A. K.: Analysis of Parallel-Operated Self-Excited Induction Generators, IEEE Trans. Energy Conversion **14** No. 2 (1999), 209-216.

[26] SANDHU, K. S.: Steady-State Analysis of Multimachine System with Self-Excited Induction Generators, Electric Power Components and Systems **34** (2006), 483–496.

[27] LEE, K. Y.—El-SHARKAWI, M. A.: Tutorial on modern Heuristic Optimization Techniques with Applications to Power Systems, IEEE Power Engineering Society, 2002, IEEE Catalog Number 02TP160.

[28] AGUSTIN, J. L. B.—LOPEZ, R. D.: Multi-Objective Design and Control of Hybrid Systems Minimizing Costs and Unmet Load, Electric Power Systems Research **79** (2009), 170–180.

[29] AZZAM, M.—MOUSA, A. A.: Using Genetic Algorithm and TOPSIS Technique for Multiobjective Reactive Power Compensation, Electric Power Systems Research **80** (2010), 675–681.

[30] El ELA, A. A. A—SPEA, S. R.: Optimal Corrective Actions for Power Systems using Multi-Objective Genetic Algorithms, Electric Power Systems Research **79** (2009), 722–733.

Received 27 July 2011

Jordan Radosavljević was born in Serbia in 1973. He received his BSc degree in 1998 from the Faculty of Electrical Engineering, University of Priština, MSc degree in 2003 from the Faculty of Electrical Engineering, University of Belgrade and PhD degree in 2009 from the Faculty of Technical Sciences, Priština University in Kosovska Mitrovica. His main research interests include power system analysis, electric power distribution and distributed power generation. Currently, he is an assistant professor with the Faculty of Technical Sciences, University of Priština in Kosovska Mitrovica.

Dardan Klimenta was born in Serbia in 1975. He received his BSc degree in 1998 from the Faculty of Electrical Engineering, University of Priština, and MSc and PhD degrees in 2001 and 2007 from the Faculty of Electrical Engineering, University of Belgrade. His main research interests include application of finite element method to power cable engineering, electric power distribution and distributed power generation. Currently, he is an assistant professor with the Faculty of Technical Sciences, University of Priština in Kosovska Mitrovica.

Miroljub Jevtić was born in Serbia in 1950. He received his BSc and MSc degrees in 1980 and 1987 from the Faculty of Electrical Engineering, University of Skopje, and two PhD degrees in 1989 and 1991, first from the Saint Petersburg State Polytechnic University, Russia, and second from the Faculty of Electrical Engineering, University of Skopje, Macedonia. His main research interests include power cable engineering, electrical insulations and distributed power generation. Currently, he is a full professor with the Faculty of Technical Sciences, University of Priština in Kosovska Mitrovica.